INSTITUTE OF BIOCHEMISTRY
SWISS FEDERAL INSTITUTE OF TECHNOLOGY ZURICH

Towards Investigation of Caveolar Endocytosis with TIRF Microscopy

Semester Work

Rolf Suter
Winter Semester 2004/05

This work was done under the supervision of Helge Ewers
in the laboratory of Prof. Dr. Ari Helenius

Abstract

Endocytosis is the process of the uptake of material into cells. There are several different pathways of endocytosis. One of these is mediated by caveolae, flask shaped invaginations of the plasma membrane. Caveolae have a protein coat which mainly consist of the integral membrane protein caveolin. Although under intense investigation, little is known about the dynamics of caveolar endocytosis.

The technique of total internal reflection fluorescence (TIRF) microscopy allows to visualize single endocytic events at the plasma membrane with a high spatial and temporal resolution. In this study we established the single components of an assay to identify interaction partners of caveolin during the first steps of the internalisation of cavoelae. Such an assay requires a fluorescent marker of caveolar endocytosis, fluorescent labeled candidate proteins for interaction and the mathematical tools to evaluate the data.

Interaction partners will transiently colocalize with caveolin 1-mRFP labeled caveolae close in time to the uptake of an individual caveolae. By TIRF microscopy, the specific uptake event can be identified by loss of caveolar fluorescence, since the caveolae do not disassemble. However, fluorescence intensity does trop as they internalize and thus leave the evanescent field. By correlation of the localization of fluorescent labeled proteins, we provide the means to identify proteins involved in this process.

Candidate proteins to be used in this assay were chosen by educated guess. Actin is involved in caveolar endocytosis. Cortactin is a actin modifying protein and therefore chosen to be used in this assay. It was labeled with enhanced green fluorescent protein (EGFP). We found that labeling did not change the intracellular distribution of cortactin. It localizes to lamellipodia, filopodia and also to some caveolin spots in form of tails. We could achieve the temporal resolution to resolve the transient recruitment of dynamin to the plasma membrane. Our findings agree with published data. We have started to investigate the kinetics of the internalisation of caveolae.

Contents

1 Introduction

1.1 Endocytosis

Nearly all eukaryotic cells use the process of endocytosis to capture extracellular molecules by enclosure within membrane vesicles or vacuoles derived from the plasma membrane. Cells use endocytosis to take up nutrients, defend themselves against pathogens and to maintain homeostasis. However, some toxins, viruses and other pathogens can abuse the endocytic pathways to enter the host cell. There exist at least five different pathways of endocytosis. Phagocytosis and macropinocytosis are used to engulf large particles and large amounts of fluid respectively. In contrast, clathrin-coated vesicles, non-clathrin coated vesicles and caveolae are small and used for ingesting fluids and solutes.

1.1.1 Phagocytosis

Phagocytosis is generally restricted to motile cells. Protozoa use this receptor-mediated endocytic process for feeding. Large particles, usually other cells, are surrounded with a portion of the flexible cell membrane and subsequently internalized and digested. The products are then used as food. In multicellular organisms phagocytosis plays an important role in host defense against pathogens. In mammals this task is carried out by white blood cells as the macrophages, neutrophiles and dendritic cells.

Phagocytosis can be divided into four steps. First, the phagocytic cell detects the particle by receptors on the cell surface to which the particle is attached. in the second step, the receptors induce a signaling process which leads to the engulfment of the particle. An outgrowing part of the plasma membrane is pushed by the actin cytoskeleton around the particle. The internalized particle which is enclosed by a former part of the plasma membrane becomes a phagosome. In the third step the phagosome matures. The surrounding actin filaments are disassembled and the phagosome is directed by microtubule-dependent motors deep into the cell. There, several fusion and fission events take place. The proteins derived from the plasma membrane are removed. In the last step the phagosome fuses with a lysosome. The fusion product is called phagolysosome. The internalized particle is digested by the lysosomal hydrolases. The small products are transported out of the phagolysosome. The remain is called a residual body.

1.1.2 Macropinocytosis

Macropinocytosis is used to internalize large amount of fluid and membrane. It is a triggered process but occurs constitutively in amoeba, thyroid cells taking up thryoglobulin and dendritic cells, which sample their environment in immune surveillance. Macropinocytosis is dependent on actin which forces the membrane to ruffle. This finally leads to large vacuoles. Some pathogens like the bacteria *Salmonella enterica* which causes food poisoning and *Salmonella typhimurium* can trigger macropinocytosis to invade the host cell.

1.1.3 Clathrin-Mediated Endocytosis

Clathrin-mediated endocytosis is a receptor mediated process which begins at clathrin-coated pits. These occupy approximatly 2 % of the total plasma membrane. Receptor-ligand complexes either induce the formation of new clathrin-coated pits or laterally move into preexisting ones. These pits consist of clathrin triskelions and adapter proteins. Clathrin is a protein complex with a three-legged structure composed of three heavy chains with each having a tightly associated light chains. Adapter or assembly proteins (AP) are responsible for targeting and transport specificity. There are at least four different AP complexes which each consist of four different polypeptides. In endocytosis the AP2 complex is targeted to the plasma membrane and mediates the assembly of the clathrin coat.

The pinching off from the plasma membrane to form clathrin-coated vesicles requires the GTPase dynamin. Dynamin self assembles around the neck of the pits. Dynamin binds to the lipid phosphatidylinositol-4,5-bisphosphate (PIP_2). This allows regulation of dynamin [1] and the association of dynamin to membranes [2].

After leaving the plasma membrane the clathrin-coated vesicles which share their structure with a soccer ball rapidly shed their coat.

1.1.4 Caveolae

Caveolae are flask shaped invaginations of the plasma membrane. Their typical size is about 50–80 nm. Caveolae are present in many cell types. Self-assembly of the integral membrane protein caveolin forms the coat of the caveolar invaginations and vesicles. Caveolin has an unusual typology in that it has an cytosolic N- and C-terminal domain which are connected with a hydrophobic sequence that is embedded in the plasma membrane but does not span it. Caveolins are palmitoylated in the C-terminus, can be phosphorylated on a tyrosin residue, can form dimers and higher oligomers and bind cholesterol with high affinity [3]. The role of caveolin in the endocytic process is not well understood. Caveolae are enriched in cholesterol, glycosphingolipids and glycosylphosphatidylinositol (GPI) anchored proteins.

The dissociation of caveolae is a triggered process which involves tyrosin phosphorylation and other signaling mechanisms. After internalization the caveolar vesicles get transported to cytoplasmatic organelles, the caveosomes.

1.1.5 Clathrin and Caveolin Independent Endocytosis

Several other pathways of endocytosis exist. It is difficult to catagorize them unambiguously. But the dependence on dynamin and lipid rafts are characteristics which help to classify these pathways. Clathrin and caveolin independent endocytosis is still poorly understood and under investigation.

1.2 TIRF Microscopy

In order to visualize endocytic events it is useful to selectively look at the plasma membrane. Fluorescence microscopy is a natural choice to trace proteins labeled with a fluorophore within a cell. Convential fluorescence microscopy illuminates the whole cell. Therefore all labeled proteins in the cell are excited. It is impossible to distinguish between proteins that are in the cytosol and such that are attached to the plasma membrane. Also, labeled proteins in the cytosol would fluoresce and make it difficult to observe the proteins attached to the plasma membrane. One microscopy technique that just excites fluorescent molecules within a defined depth in the cell is confocal microscopy. However, even these confocal slices which have a depth of 500–1000 nm are to thick to resolve the dynamics of the small endocytic vesicles of a diameter of about 100 nm. Confocal microscopy is also to slow to resolve the endocytic dynamics and causes fast bleaching of the fluorescent molecules.

Total internal reflection fluorescence (TIRF) microscopy (also called evanescent field (EF) fluorescence microscopy) overcomes these problems (for review see [4, 5]). It allows the selective excitation of fluorophores in an aqueous or cellular environment very near a solid surface (within $\geq$ 100 nm). Fluorophores farther away from the surface are not excited. This feature of TIRF microscopy allows the study of the endocytic event.

1.2.1 Theory of TIRF

The thin layer of illumination is an evanescent field which forms when a beam of light traveling in a medium with a high refractive index, like glass, (n_{glass}) encounters one of low refractive index such as water (n_{liquid}). When the critical angle of incident θ_c, measured from the normal, is large enough, the beam undergoes total internal reflection (TIR). This means, that the light does not cross the interface glass/water. Instead it is reflected. Classical electrodynamics do not allow an electromagnetic wave to dissappear discountinuously at an interface. Therefore TIR generates a very thin electromagnetic field in the liquid, the evanescent field, which oscillates with the same frequency as the insident light. The intensity of the evanescent field decreases exponentially with the distance to the interface. The critical angle θ_c can be calculated from:

$$\theta_c = \sin^{-1}\left(\frac{n_{liquid}}{n_{glass}}\right) \tag{1}$$

1.2.2 Optical Configurations

In general there are two ways to build up a TIRF microscope. The light, usually from a laser with a total visible ouput in the 100 mW range, which generates the evanescent field can either be directed through a prism to the TIR interface or through a high numerical aperture (NA $>$ 1.4) microscope objective itself (Figure 1).

TIRF with a Prism Using a prism can be an inexpensive and easy way to set up a TIRF microscope. A prism based TIRF microscope can illuminate a larger area. This

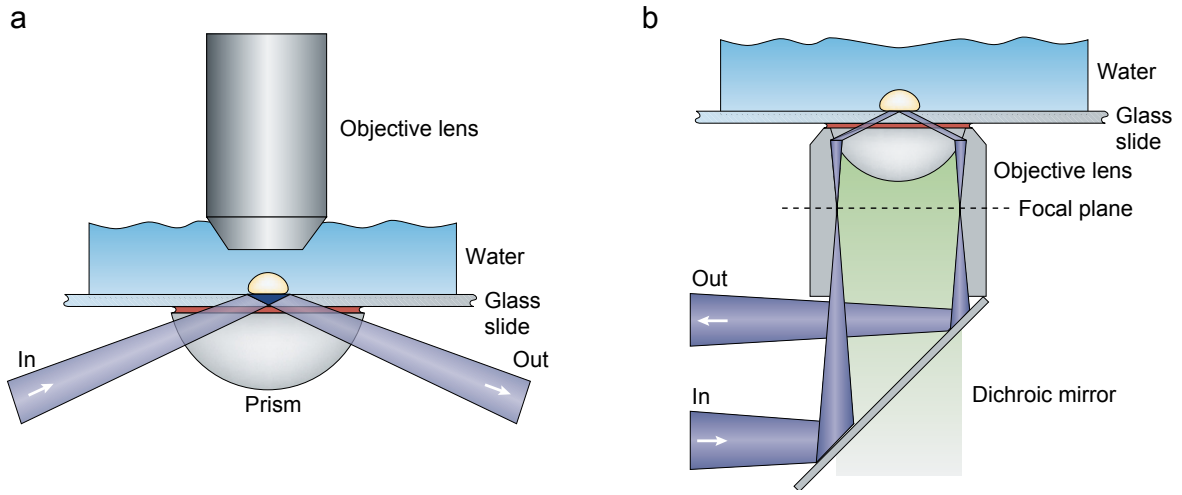

Figure 1: Two types of TIRF microscope. (a) A prism-type TIRF microscope. (b) Outline of a through-the-lens TIRF microscope.

can be an advantage when visualizing several cells or cells that are spread over a large area. Depending on the exact configuration, the sample has to be sandwiched into a narrow space between the prism and the objective. This makes it difficult to access the sample.

Prismless TIR through the Objective Through-the-lens TIRF microscopes allow free access to the sample. They also give a higher image quality and spatial resolution. However, the illumination is not pure. Scattered light and luminescence from the objective also contribute to the illumination of the sample.

The high angle of incident light can be achieved when the light beam is introduced off-axis into the objective (Figure 1 b). The NA of the objective must be substantly greater than n_{liquid}. Using a NA $= 1.4$ objective and water with $n_{liquid} = 1.33$ the required conditions are fullfilled. But when viewing at a cell at $n_{liquid} = 1.38$ the TIR is just above the critical angle which leads to a deep evenescent field. Some dense organelles then would convert some of the evenescent field into scattered light which gives a poor resolution.

1.3 Aim of this Project

The caveolar pathway of endocytosis has been studied previously (for review see [3]). But up to now little is known about the dynamics of caveolar endocytosis. Also the temporal interplay of endocytic factors during the internalization of caveolae is not well understood.

Earlier work [6, 7] examined the temporal aspects of clathrin-mediated endocytosis using TIRF microscopy. In those studies fluorescently labeled clathrin was imaged

together with labeled candidate protein on a TIRF microscope.

The aim of this project is to set up the single components of an assay to investigate caveolar endocytosis using TIRF microscopy. Potential interaction partners had to be identified and labeled with a fluorophore. Experience with the TIRF microscope had to be aquired. We had to prove whether we can achieve the temporal resolution required to resolve endocytic processes. The mathematical tools to process the data were also needed. And finally we had to characterize the internalization of caveolae.

2 Materials and Methods

2.1 Materials

2.1.1 Media for Cell Culture

MEMα	32561-029	Gibco Life Techn.
CO_2 independent medium	18045-054	Gibco Life Techn.
Trypsin, EDTA (1×)	25300-054	Gibco Life Techn.

2.1.2 Cells

DH5α		
HeLa		ATCC
HeLa Cav1-mRFP		Arnold Hayer

2.1.3 Plasmids and Oligonucleotides

flag cttn wt		Parsons' Laboratory [8]
flag cttn W22A		Parsons' Laboratory
flag cttn W525K		Parsons' Laboratory [8]
pEGFP-N1	6085-1	Clontech

All oligonucleotides were synthesized by Microsynth.

2.1.4 Enzymes

Pfu Turbo DNA polymerase	600250-52	Stratagene
BamHI	R0136S	New England Biolabs
EcoRV	R0195S	New England Biolabs
NotI	R0189S	New England Biolabs
NotI	E0304Y	Amersham Bioscience
KpnI	R0142S	New England Biolabs
XhoI	R0146S	New England Biolabs
T4 DNA ligase	#EL0011	Fermentas

2.1.5 Kits for Transfection, Cloning and DNA Purification

Cell Line Nucleofector Kit R	VCA-1001	Amaxa
MinElute PCR Purification Kit	28004	Quiagen
Gen Elute Plasmid Miniprep Kit	PLN70	Sigma
Nucleospin Plasmid	740588.250	Macherey-Nagel
Jetstar 2.0 Plasmid Maxiprep Kit	220020	Genomed

2.1.6 Antibodies

anti caveolin-1 (rabbit)	sc-894	Santa Cruz
anti cortactin (mouse)	05-180	Upstate
anti EEA1 (rabbit)	ab2900	Abcam
goat anti mouse IgG Af-594	A-11005	Molecular Probes
goat anti mouse IgG Af-647	A-21236	Molecular Probes
goat anti rabbit IgG Af-488	A-11008	Molecular Probes
goat anti rabbit IgG Af-594	A-11012	Molecular Probes
goat anti rabbit IgG Af-647	A-21245	Molecular Probes

2.1.7 Others

LE Agarose	50004	SeaKem
1 kB DNA ladder	#SM0311	Fermentas
Vanadate (Na_3O_4V)		
Geneticin G-418 Sulphate	11811-031	Gibco

2.2 Equipment

2.2.1 Conventional Fluorescence Microscope

Inverted Microscope	Axiovert 100 M	Zeiss
Charge-coupled-device (CCD) camera	C4742-95	Hamamatsu

2.2.2 TIRF Microscope

Inverted Microscope	IX-71	Olympus
PlanApo 60×/1.45 Oil objective		Olympus
He-Ar laser	BeamLok	Spectra-Physics
Camera	Imageo-QE	TILL Photonics

2.3 Software

Openlab 3.1.2	Improvision
TILLvisION 4.0	TILL Photonics
ImageJ 1.32	NIH
Excel	Microsoft

2.4 Methods

2.4.1 Cloning

Polymerase Chain Reaction (PCR) In order to amplify the cortactin gene and to introduce new restriction sites a polymerase chain reaction (PCR) was performed. PCR was done on a Mastercycler personal (Eppendorf). The program used on the

PCR machine is shown in Table 1. PCR products were purified with a QIAquick PCR Purification Kit. The composition of the reaction mixture is noted below.

5 μl	10× Cloned Pfu Reaction Buffer	(10×)
1 μl	dNTP 10 mM (each)	(0.2 mM)
1 μl	primer 1	(0.2 μM)
1 μl	primer 2	(0.2 μM)
1 μl	DNA template (10 ng/μl)	(10 ng)
40 μl	ddH_2O	
1 μl	Pfu Turbo DNA polymerase	
50 μl	total volume	

Restriction Digest Standard protocols were used for restriction digests. The preperative restriction digests were performed in a total volume of 50 μl. For analytical digests, a volume of 10 μl was used. The rections were incubated at 37 °C for at least 1 h.

Ligation The concentrations of the insert and target vector were estimated by comparing the bands on a 0.9 % agarose gel with those of the marker. The ligation rections were performed in a total volume of 20 μl and not more than a total amount of 150 ng DNA was used. The molar ratio of vector to insert varied between 1:7 and 1:12. For ligation, 2 μl 10× ligation buffer and 5 Weiss-units of T4 DNA-ligase (1 μl) were added to the mixture of vector and insert. The ligation mix was then incubated for at least 1 h at room temperature.

Transformation 10 μl of the ligation were pipetted into an Eppendorf tube and put on ice. 30 μl of chemically competent *E. coli* DH5α were added and incubated for 30 min on ice. The mixture was then heated to 42 °C for 90 seconds and put back on ice for 2 min. Then 1 ml of 37 °C prewarmed Luria Broth(LB)-media was added and the cells were shaken at 37 °C for 30–60 min. The bacteria were spun down in a microcentrifuge at 16 100 × g for 1 min, resuspended in 1 ml of fresh media and diluted 1:10, 1:100 and 1:1000. Finally the bacteria were plated on LB-plates with ampicillin. The bacteria

initial denaturing	95 °C	2 min
denaturing	95 °C	45 sec
annealing	57 °C	45 sec
elongation	72 °C	2 min
30 cycles		
final elongation	70 °C	10 min
samples were cooled to 4 °C		

Table 1: Program used for PCR.

solution were distributed with small glass spheres. The plates were then put to 37 °C over night. Clones were selected the day after.

Plasmid Preparation Transformed *E. coli* DH5α bacteria were grown in LB-media supplemented with 100 μg/ml ampicillin. DNA minipreps were made from 4 ml of cell culture with NucleoSpin Plasmid kit from Macherey-Nagel. The DNA was finally eluted in 30 μl water.

DNA maxipreps of constructs were done with the Jetstar 2.0 Plasmid Maxiprep Kit from Genomed. A total of 150 ml of an overnight cell culture was harvested. The DNA was eluted in 400 μl 5 mM Tris/HCl (pH 8.5). The DNA concentration was determined by diluting the DNA 1:100 and measureing the absorbance at 260 nm.

DNA Analysis

Gel Electrophoresis DNA fragments were analyzed on an 0.9 % agarose gel by gel electrophoresis. The gel was produced by heating up a solution of 60 ml TAE and 0.54 g agarose in a microwave oven. The solution was then poured into the pouring unit. After setting the comb 3 μl ethidium bromide solution was added under the hood. The DNA samples were supplemented with 2 μl DNA loading buffer and then filled up with ddH_2O to a total volume of 10 μl. After loading the samples to the gel it was run with a constant current of 85 mA for 50 minutes.

DNA Sequencing The samples from which the nucleotide sequence had to be known were sequenced at Synergene. The DNA was diluted with ddH_2O to a concentration of 150 ng/μl in a total volume of 10–15 μl. When it was required to use costum sequencing primers 1 μl primer (10 pmol/μl) was added. The samples were sent out in 200 μl PCR tubes.

2.4.2 Cell Culture

HeLa cells were obtained from the American Type Culture Collection (ATCC). The HeLa Cav1-mRFP cells stably expressing caveolin 1-mRFP were produced by Arnold Hayer. Cells were maintained in 10-cm Petri dishes at 5 % CO_2 in MEMα supplemented with 10 % fetal calf serum (FCS) and 1× nonessential amino acids (NEAA). To keep the HeLa Cav1-mRFP cells under selective pressure, 100 μl of a geneticin solution (50 mg/ml in 10 mM HEPES) was added to the medium.

Cells used for microscopy were grown on 18 mm coverslips. For imaging the coverslips were mounted in the imaging chamber which was filled with 1 ml CO_2 independent medium. All imaging was performed at 37 °C.

2.4.3 Transfection

To introduce plasmid DNA into HeLa and HeLa Cav1-mRFP cells they were transfected with a Nucleofactor Kit R (Amaxa). Cells of a nearly confluent 10 cm dish were first

washed and then trypsinized with 2 ml trypsin solution for several minutes. Then 8 ml medium (MEMα + 10 % FCS + 1× NEAA) were added to the trypsinized cells. The cells were singularized by pipetting and an aliquot of 1.5 ml of this cell solution was then centrifuged in an Eppendorf tube for 10 min at 210 × g. Meanwhile a 12-well plate was prepared with a coverslip and 1 ml medium (MEMα + 10 % FCS + 1× NEAA) each in four wells. Also an additional Eppendorf tube was filled with 0.5 ml medium. After centrifugation, the supernatant was removed and the cells were resuspended in 100 μl Nucleofactor Solution R. 2 μg DNA were added and the whole solution was transfered to an electroporation cuvette. Immediatly after electroporatoin with programm I-13, the cells were equally distributed to the four coverslips in the 12-well plate.

2.4.4 Antibody Staining

Cells were fixed for 20 min with either 0.5 ml 4 % paraformaldehyde in serum free media or 0.5 ml 4 % formaldehyde in PBS. Then the cells were washed with PBS and quenched for 5 min with PBS/glycin 50 mM. The dilution buffer for antibodies was composed of PBS, 1 % BSA, 0.05 % saponin, 0.02 % NaN_3. After quenching, the cells were blocked for 45 min with 4 % goat serum in dilution buffer. Coverslips were then transfered to an humidity chamber. The primary antibody, which was diluted with dilution buffer, was added and incubated for 2 h at room temperature. Then the primary antibody was exchanged against the secondary antibody, diluted 1:500 with dilution buffer. After incubation for 30 min at room temperature, the coverslips were washed with PBS and water by dipping them into the required solution. Finally, the coverslips were mounted with Immu-Mount (Thermo) and nail polish on a microscope slide.

2.4.5 Fluorescence Microscopy

Fixed Cells All fixed cells were viewed on a Zeiss Axiovert 100 M inverted microscope. For GFP constructs the typical settings were: 100×/1.40 Oil DIC Apochromat objective, 10–20 % gain, 0 % offset, 500–800 ms exposure time and 2× binning. For antibody stained cells the levels of gain, offset and the exposure time were adjusted. Images were taken with the Openlab 3.1.2 software.

TIRF Microscopy For TIRF microscopy, transfected cells on a 18 mm coverslip were mounted in a custom-built ring and covered with 1 ml CO_2 independent medium. This ring was put onto the stage of the microscope, which was surrounded by a heated (37 °C) acrylic glass chamber. TIRF microscopy was done with the Olympus 60× objective. Fluorophores were excited by the evanescent field caused by a laser beam introduced through the objective. GFP and RFP constructs were excited with the 488 nm and the 568 nm laser line of the He-Ar laser respectively. Imaging was done with the TILLvisION 4.0 software. Videos were made with a frame rate of 0.5 Hz. Up to 400 frames were collected. To image the single frames, GFP and RFP constructs were excited sequentially with an exposure time of 200 ms. Cells on one coverslip were imaged for a maximum of 90 min.

2.4.6 Image Processing and Data Analysis

Image Processing Images of fixed cells were exported from the Openlab software in a 12 bit greyscale TIFF format. These files were further processed with Photoshop 7.

Video Processing Greyscale videos taken with the TILLvisION software were exported as avi files with a Microsoft RLE compression, set the compression quality to 100 %. For analysing the videos, they were imported with the Quicktime plugin into ImageJ.

3 Results

3.1 Requirements for an Assay

To visualize molecules with TIRF microscopy, as with conventional fluorescence microscopy, they have to be tagged with a fluorophore. This can be done by cloning a fluorescent protein, like green fluorescent protein (GFP), into the coding sequence of the gene of interest. There are several different fluorophores available which can be used to distinguish between molecules. To investigate caveolar endocytosis a marker for this pathway is needed. It is also required to prove that the spatial and temporal aspects of endocytosis can be resolved. And last but not least the mathematical tools to evaluate the data had to be acquired.

3.2 Choosing Molecules to Investigate

As a marker of caveolar endocytosis we chose caveolin 1 (Cav1). HeLa Cav1-mRFP cells express caveolin 1, labeled with monomeric fluorescent protein (mRFP). These cells were obtained from Arnold Hayer. Possible interaction partners were selected by educated guess from the literature.

Dynamin 2 is transiently recruited in simian virus 40 (SV40) induced internalization of caveolea [9]. Actin is involved in several known pathways of endocytosis. Bursts of actin polymeriuation (tails) have been found in caveolar endocytosis [9]. Actin related protein 3 (Arp3) is a component of the Arp2/3 complex which is required for actin polymerization. Cortactin (Cttn) which interacts with Arp3, dynamin, N-WASP and F-actin is a protein likely to be involved in caveolar endocytosis [2, 10].

3.2.1 Cortactin

Cortactin is a rod shaped protein which consist of a N-terminal acidic Domain (NTA) followed by F-actin-binding repeats, an α helical domain, a prolin/tyrosine rich domain and a C-terminal Src homology (SH3) domain (Figure 2). Human, rodent and avian cortactin share high sequence similarity [10].

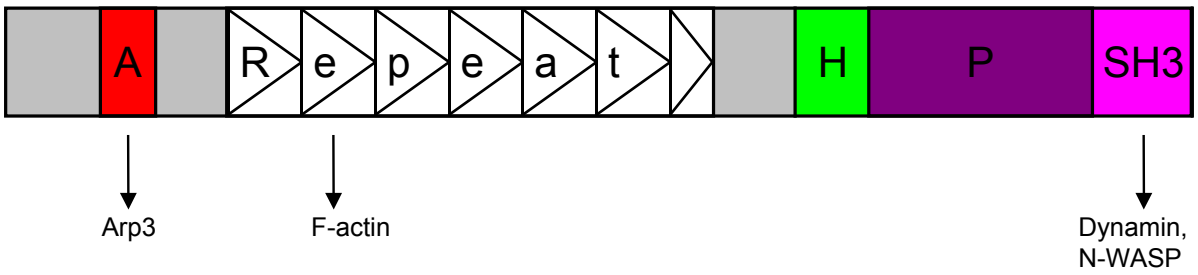

Figure 2: Domain structure of cortactin. A, acidic domain; H, helical domain; P, proline-rich domain.

The NTA contains a conserved acidic, tryptophan containing motif DDW. This motif mediates the binding to Arp3. Mutation of both acidic residues or the tryptophan inhibit the interaction with Arp3. The F-actin-binding domain is built from 6.5 tandem copies of a 37 amino acid repeat. There are two isoforms of cortactin which lack the sixth or the fifth and the sixth repeat respectively. These isoforms have a lower binding affinity to F-actin. They are derived by alternative splicing of the mRNA. Looking at the C-terminal half of the protein, the exact role of the α helical domain is rather unknown. The prolin-rich domain mediates interaction with specific tyrosin kinases. The SH3 domain is reponsible for the interaction with prolin/arginin rich domains of dynamin, WASP and other proteins. This can be disrupted by a mutation of a tryptophan residue within this domain.

3.3 Cortactin-EGFP Constructs

Cortactin wt, W22A and W525K clones originated from J. T. Parsons' laboratory [8]. The cortactin W22A mutant has a change in the DDW motif of the NTA and therefore the binding to Arp3 is inhibited. The cortactin W525K mutant has a disrupted binding site to dynamin, WASP and other SH3 target proteins. These clones were optained in a flag tagged form inserted into a pcDNA3 plasmid (Invitrogen).

To verify the coding sequence of the DNA we recived, we sent the plasmids with the three different clones out for sequencing. As sequencing primers we chose 5´-TAA TAC GAC TCA CTA TAG GG-3´ (T7) and 5´-TAG AAG GCA CAG TCG AGG-3´ (pcDNA3.1rev) supplied from Synergene and 5´-GAC GGA GAA GCA TGA GTC TCA G-3´ (cttn_seq_midf) which was orderd from Microsynth. The nucleotide sequences we got back were overlapping and showed a clear separation of the signal peaks. We performed a BLAST search with the nucleotide sequences. The nucleotide sequence of our clones match exactly with Mus musculus cortactin (Cttn), mRNA [gi:6681086]. The cortactin mutants W22A and W525K have the expected mutations. No other mutations were introduced.

DNA fragments encoding cortactin and mutants were prepared by PCR using the obtained plasmids as templates. The primers used in PCR were 5´-CGA TCT CGA GAT GTG GAA AGC CTC TGC AGG-3´ (cttn-5´) and 5´-CGT AGG ATC CAA CTG CCG CAG CTC CAC ATA G-3´ (cttn-3´). These primers introduced a XhoI site and a BamHI site at the regions corresponding to the N-terminus and C-terminus, respectively. The 3´-primer (cttn-3´) also removed the stop codon. After purifying the resultant PCR products with a MinElute PCR Purification Kit we digested them with XhoI and BamHI. As a target vector we used pEGFP-N1, which was also cut with XhoI and BamHI. Vector and insert were then purified with the MinElute PCR Purification Kit. We ligated the inserts into the vector and transformed *E. coli* DH5α with the ligation product. Bacteria were diluted 1:10, 1:100 and 1:1000 and then plated on LB-plates with ampicillin for selection. Next day, we chose three clones of each ligation reaction from the plates with the highest dilution of the bacteria that showed clones. These clones were cultured in 5 ml LB-medium with ampicillin over night. From this cultures we made DNA minipreps to isolate the cortactin-EGFP encoding plasmids. To prove if

the cortactin fragment has really been inserted into the vector, we made an analytical digest with XhoI and NotI. If the cortactin had really been inserted, we should get a small fragment of 2.4 kb (cortactin-EGFP) and a large fragment of 3.9 kb of the remain or the plasmid. On the other hand, if the cortactin had not been inserted, we get a small fragment of 0.7 kb (EGFP) and the remain of the plasmid would still be 3.9 kb. This digest was then run on an analytical 0.9 % agarose gel (Figure 3 a). Only Cttn-EGFP wt 1 and 2 (lane 7 and 8) showed the 2.4 kb fragment. This means that only these two clones have a plasmid with an incorporated cortactin gene fragment. All other clones (Cttn-EGFP wt 3, Cttn-EGFP W22A 1-3 and Cttn-EGFP W525K 1-3) in lane 9 through 15 have a band of a small 0.7 kb DNA fragment which represents the EGFP fragment without an incorporated cortactin gene.

Because the construction of the cortactin-EGFP W22A and W525K failed, we repeated the cloning for this mutants. The PCR products were redigested with XhoI and BamHI and again purified with the MinElute PCR Purification Kit. Then, they were ligated again into the already cut and purified vector pEGFP-N1. *E. coli* DH5α were transformed with the ligation product and plated as before. We chose four and six colonies of the cortactin-EGFP W22A and W525K clones respectively, cultured them in 5 ml LB-medium with ampicillin over night and made DNA minipreps the next day. As before, we made an analytical digest of the purified plasmids with XhoI and NotI and run an analytical 0.9 % agarose gel (Figure 3 b). Cttn-EGFP W22A 4, Cttn-EGFP W525K 1 and 5 showed the 2.4 kb cortactin-EGFP fragment (lane 9, 10 and 14). All other clones (lane 6–8, 11–13 and 15) have no cortactin insert.

To get more cortactin-EGFP DNA we performed a DNA maxiprep. For this, the colonies of the clones, which have the insert (Cttn-EGFP wt 1, Cttn-EGFP W22A 4 and Cttn-EGFP W525K 1) and were stored at 4 °C, were picked again and cultured in 150 ml LB-medium with ampicillin. After incubation over night, we harvested the bacteria and isolated the plasmids with the Jetstar 2.0 Plasmid Maxiprep Kit. To ensure that we have picked the right clones and not have mixed them up, we made an analytical digest with XhoI and NotI as used before. We also sent the clones our for sequencing to Synergene. All clones contained the cortactin gene fragement. Sequencing also showed that we have not mixed up the clones and that no additional mutation was introduced by accident.

3.4 Localization of Cortactin

To check the distribution of endogenous cortactin we stained HeLa ATCC cells with antibodies against cortactin (Figure 4). The micrographs show that cortactin is localized in spots distributed throughout the cytoplasma. It is accumulated at the edges of the plasma membrane in filopodia and lamellipodia and also in focal adhesion contacts. In general, cortactin is located to places, where a dense actin network undergoes rearrangements.

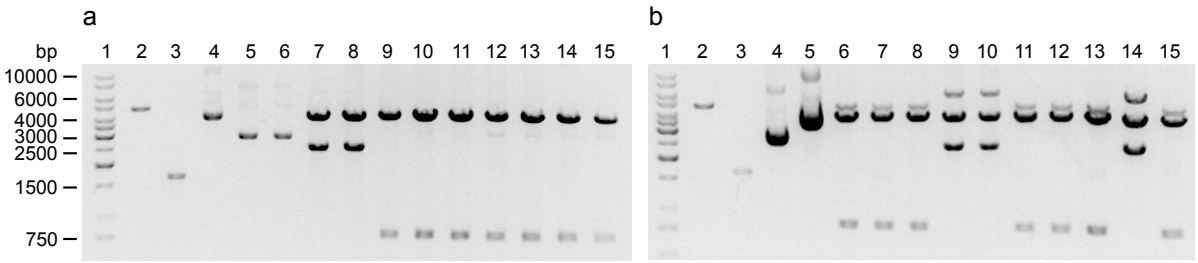

Figure 3: Analytical restriction digest. The Cttn-EGFP wt/W22A/W525K clones were isolated with a miniprep kit. Samples were digested with XhoI and NotI. The resulting fragments were separated on a 0.9 % agarose gel: lanes 7 and 8 (a) and 9, 10 and 14 (b) show a band at 2.4 kb which indicates the incorporation of the insert. 1 kb DNA ladder: Lane 1 (a, b). Digested target vector: Lane 2 (a, b). Cortactin insert: Lane 3 (a, b). Undigested clones: Lanes 4–6 (a) and 4, 5 (b). Digested Cttn-EGFP wt: lanes 7–9 (a). Digested Cttn-EGFP W22A: lanes 10–12 (a) and 6–9 (b). Digested Cttn-EGFP W525K: lanes 13–15 (a) and 10–15 (b).

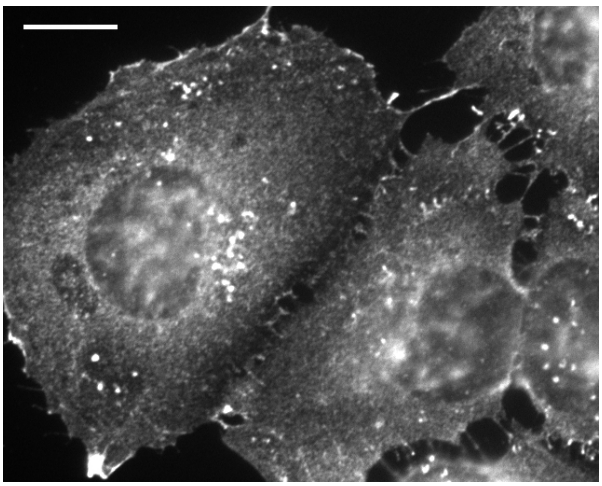

Figure 4: Localization of Cortactin. HeLa cells stained with an anti-cortactin antibody. Scale bar represents 10 μm.

3.5 Testing Cortactin-EGFP Constructs

To verify that the cloned Cortactin-EGFP constructs (Cttn-EGFP wt, W22A and W525K) localize correctly, we transfected HeLa AtCC cells with these contstructs. Cells were fixed and stained with antibodies against cortactin. Fluorescent micrographs show that the overall distribution of cortactin was not altered by expression of cortactin-EGFP. However, we observed a perinuclear accumulation of cortactin-EGFP that was not stained by the anti cortactin antibody. Cells transfected with cortactin-EGFP W525K have a lower viability than those transfected with cortactin-EGFP wt.

3.6 Colocalization of Cortactin with Caveolin

To score for colocalization of caveolin and cortactin, we transfected HeLa Cav1-mRFP cells with cortactin-EGFP. Fluorescence micrographs of fixed cells show that some caveolin spots have tails of cortacin (Figure 6). This strengthens our hypothesis of the involvement of cortactin in caveolar endocytosis.

3.7 Setting up a TIRF-Microscopy based Assay

Caveolae stay at the plasma membrane until their internalization is triggered [11]. Caveolae do not disassemble during internalization. When observing caveolar endocytosis with a TIRF microscope, the endocytic vesicles move out of the evanescent field and therefore their fluorescence intesity decreases. This event would be observed as a disappearance of a spot in a sequence of several images.

Several proteins are transiently recruited to the site of caveolar endocytosis. When using two different colors to label a caveolar marker like caveolin and a candidate protein, it is possible to trace these two molecules simultaneously. The fluorescence intensity of labeled candidate proteins is thought to show a transiently appearing spot at the endocytic site. Measuring the fluorescence intensity and the position of the two spots would allow the characterization of the spatial and temporal relationship between the labeled proteins.

3.8 Recruitment of Dynamin to the Plasma Membrane

To improve the microscope technique and to gain first experience in data analysis we chose dynamin 2 and caveolin 1 to try to score for events. We transfected HeLa Cav1-mRFP cells with dynamin 2-GFP. Next day we acquired videos on the TIRF microscope. To stimulate caveolar endocytosis we incubated the cells with 1 mM ortho-vanadate (Na_3O_4V) [9]. Dynamin 2-GFP and caveolin 1-mRFP were excited sequentially with the 488 nm and the 568 nm laser lines through TIR illumination for 200 ms. The image rate was 0.5 Hz. Fluorescence emission was collected through a dual band filter for both channels.

The intensity of the videos was adjusted automatically. Videos were exported in a quicktime format for data processing. These videos were then imported in a 8 bit

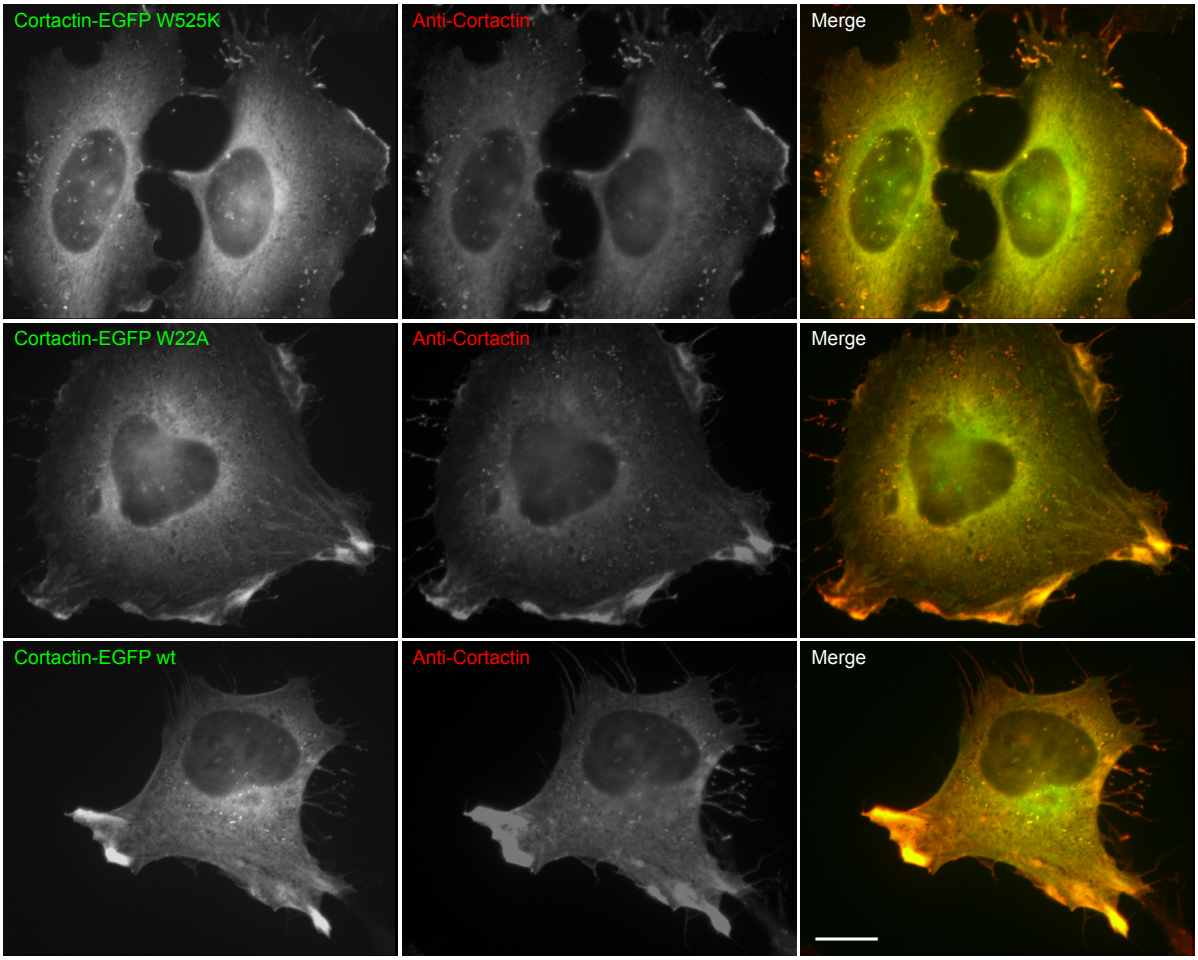

Figure 5: Testing cortactin-EGFP constructs. HeLa cells transfected with cortactin-EGFP wt, W22A and W525K, respectively. Cells were stained with an anti-cortactin antibody. Scale bar represents 10 μm.

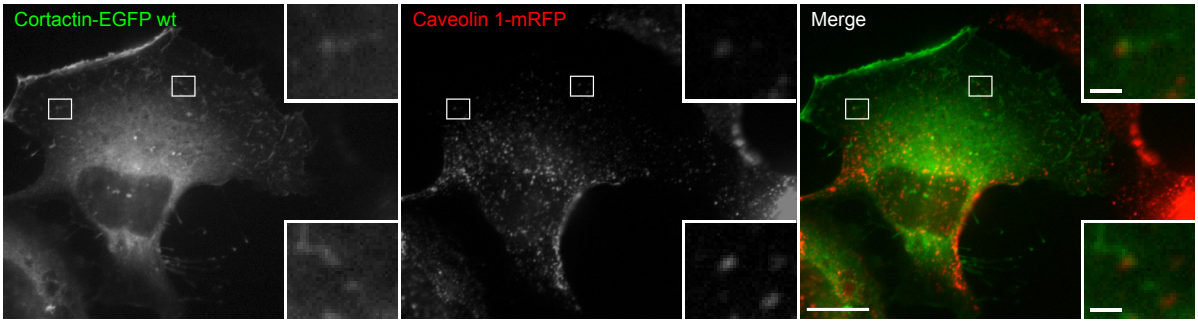

Figure 6: HeLa Cav1-mRFP cell transfected with cortactin-EGFP wt. Scale bars represent 10 μm and 1 μm (enlargements).

greyscale mode into ImageJ. To get a fast impression if dynamin is colocalizing with caveolin, we simply merged the dynamin and the caveolin channel to a RGB video. Then we screened for yellow spots which indicate the presence of dynamin and caveolin. We also searched for dynamin spots which are temporarly recruited to caveolae. However, we did not find such events. Facing this problem, we decided to look at the single molecules first. Because the signal to noise ratio of the caveolin signal was low, we chose dynamin to evaluate first.

The movies of the dynamin signal allowed to look at single dynamin spots. These spots were more or less clearly separated dots. In general we can divide these dots into two categories. The first group includes spots that are stationary or move slowly. The other group encloses dots that appear transiently. We call these second group blinking events, because of their short appearance. To evaluate these blinking events, we chose only such dots, that do not move laterally. We draw a circle with a diameter of 4–8 pixels (320–640 nm) around such a stationary blinking dots. Then we ran a makro within ImageJ which calculated the mean intensity within this circle for every single frame of the movie. To correct for background, we ran the macro on a circle with background signal. The data of these two measurements were then copied into an Excel sheet for further data analysis. To correct for the background, we subtracted from every single mean value of the signal series the corresponding mean value of the background series (Figure 7 a). We measured several of such events. We overlaid multiple curves relative to their absolute peaks. Then we calculated the mean and standard deviation of the intensity values of these curves for each timepoint (Figure 7 b). Our data show that dynamin is temporarily recruited to the plasma membrane. The assembled intensity curve of several blinking events fits to previously published data [6].The whole process of appearance and disappearance takes approximately 80 seconds. The intensity maximum is reached in 2–3 seconds.

3.9 Detecting Internalization of Caveolae

We aimed at getting an impression of the endocytic entry of caveolae. Therefore we aquired videos of live HeLa Cav1-mRFP cells transfected with Arp3-EGFP with the TIRF microscope. We imaged cells in TIRF and epifluorescence mode simultanously. The cell was first exposed to TIR illumination for 200 ms for each channel and then the epifluorescence images were taken for both channels. The frame rate was 0.5 Hz as before. Then we analysed the recorded movie with ImageJ. To qualify the entry of caveolae, we merged the TIRF and the epifluorescence movie of caveolin 1-mRFP. We assigned the grey values of the epifluorescence movie to the red channel and those of the TIRF movie to the green channel of a RGB movie. Caveolin 1-mRFP containing vesicles attached to the plasma membrane will fluoresce under both, TIR and epi illumination. In the RGB movie with artificial colors it appears yellow. As soon as it pinches off the plasma membrane, it will turn red because it is then only visible in the epifluorescence movie. We screened for such events and found them (Figure 8).

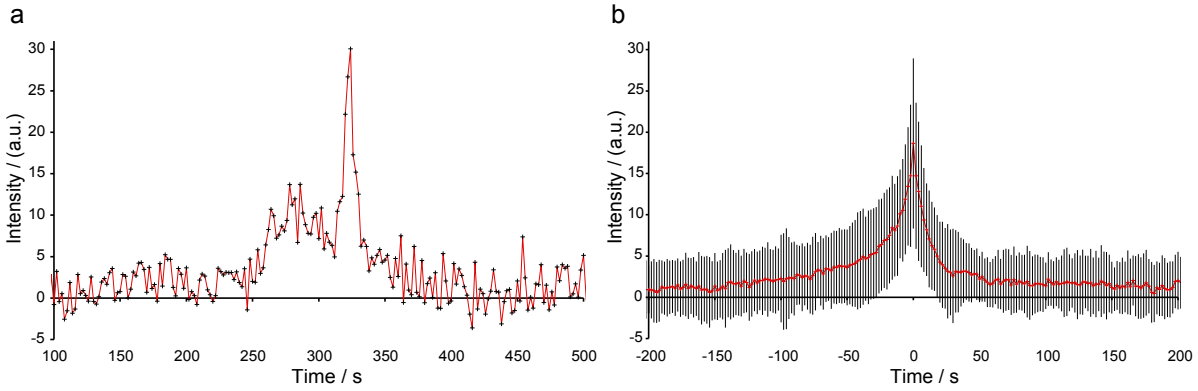

Figure 7: Recruitment of dynamin to the plasma membrane. (a) Fluorescence intensity of a dynamin blink observed with a TIRF microscope plotted against time. The mean intensity within a circle surrounding the blinking event was measured. The intensity was corrected for background by subtraction of the mean intensity of an area of similar size for every timepoint. Time origin represents the beginning of the video recording. (b) Average of multiple dynamin blinking events. The timepoint of the intensity maximum of the single measurements (a) were set to 0 s. The average of 43 events was calculated for every timepoint. Error bars represent the standard deviation.

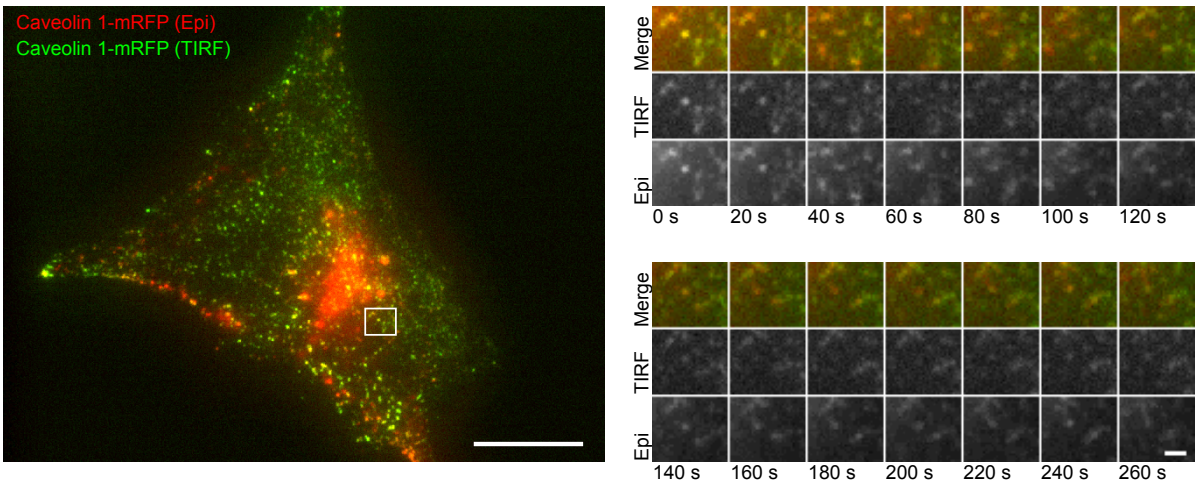

Figure 8: Internalization of caveolin. Live fluorescence recordings of HeLa Cav1-mRFP cells transfected with Arp3-EGFP. Alternating epifluorescence and TIRF images of caveolin and Arp3 were taken. The left panel shows the superimposition of a epifluorescence image (red) and a TIRF image (green) of cavoelin 1-mRFP. Right panels show time series of the region outlined as a white rectangular in the left panel. Scale bars represent 10 μm (left panel) and 0.8 μm (enlargement).

4 Discussion

4.1 Construction of Cortactin-EGFP

The analytical digest of the pEGFP-N1 plasmids showed that few clones incorporated a cortactin gene fragment. This might be due to a low efficiency of the ligation.

4.1.1 Low Ligation Efficiency

There are several possible explanations for the low ligation efficiency. It may be that the restriction digest of the vector pEGFP-N1 or the insert with the cortactin gene was inefficient. As the ligation of pEGFP-N1 cortactin wt construct worked, the digestion of the vector must have at least partly worked. So it might still be, that the digestion of the insert failed. As we pipetted the restriction digest reactions in three individual tubes separately, it is possible that we forgot one component or used the wrong amount. Another possibility is the enzymes were to some extent denatured and therefore inactivated. It could also be that the enzymes could not work properly because there were only few nucleotides between the end of the PCR fragment and the restriction sites. As we did not dephosphorylate the 3´-ends of the cut vector, it may be that the vector just ligated better back to itself than with the insert, although the restriction sites were not complementary. It is also possible that the ligation just did not work properly. As we pipetted also this reaction in three individual tubes it is also possible that we just forgot one component. It also might be that the ligase did not work correctly.

4.2 Anti Cortactin Staining and Cortactin-EGFP

As already mentioned, there are some discrepancies between the distribution of the anti cortactin antibody and the cortactin-EGFP. In filopodia and lamellipodia we can observe that the signal of antibody staining is higher signal than that of cortactin-EGFP. In opposite, the cortactin-EGFP is localized more in the region of the endoplasmatic reticulum.

An explanation for this observation might be that the antibody does not recognize the unfolded cortactin in the endoplasmatic reticulum. Because EGFP is a very stable protein, it could be that the EGFP part of the fusion protein is folded correctly and therefore is seen in the endoplasmatic reticulum, whereas the cortactin part is not folded properly and could not be detected by the antibody. This unproper folding can be caused by the short linker between cortactin and EGFP, which is shorter than that used in other studies [12] or it is due to overexpression and an accumulation of cortactin-EGFP in the endoplasmatic reticulum.

4.3 Cortactin Colocalizes with Caveolin

We studied colocalization of cortactin-EGFP and caveolin 1-mRFP in HeLa cells. Caveolin spots that have tails of cortactin were observed. There are also patches in the

perinuclear region which have signal in both channels. However, it is unlikely that cortactin and caveolin colocalize at these patches. In these regions it seems that the cortactin is mainly located in the endoplasmatic reticulum (ER) whereas caveolin is located near the plasma membrane. So the proteins would be located to different planes. To achieve higher resolution of colocalization, it would be desirable to use a confocal microscope instead of a conventional epifluorescence microscope.

4.4 Stimulation of Caveolar Endocytosis

For live cell TIRF microscopy we stimulated caveolar endocytosis with 1 mM orthovanadate (Na_3O_4V), a vanadium oxide. It inhibits ATPase, alkine phosphatase and tyrosin phosphatase. Ortho-vanadate enhances initial binding of SV40 to cells and increases caveolin dependent uptake of virus beyond a single cycle [9]. SV40 triggers local tyrosin phosphorylation in caveolae. Phosphatases reverse this process by removing the phosphate group from the tyrosines. It is thought that inhibiting these phosphatases with ortho-vanadate causes the same effect as phosphorylation by SV40 induced kinases.

We tried to quantify the number of blinking events and stationary spots of caveolin and dynamin during a specified time span in stimulated and unstimulated cells. However, we were not able to find significant differences between the stimulated and nonstimulated cells. Additionally, there were big differences within the group of stimulated and also within the group of unstimulated cells. An explanation for the failure might be that the choice of the area was to a certain extent biased. The areas were probably to small and therefore we did not count a sufficent amount of events.

4.5 Recruitment of Dynamin to the Plasma Membrane

Our results clearly show that dynamin is transiently recruited to the plasma membrane. There are two phenotypes of dynamin at the plasma membrane. The first one includes the dynamin which is stationary or moves slowly lateraly at the plasma membrane. The spots of this phenotype are visible on the plasma membrane for a long time. The other phenotype covers the blinking events, which are dynamin spots temporarely recruited to the plasma membrane. As nearly no dynamin spot colocalize with caveolin we can not deduce a role in caveolar endocytosis. The assembled intensity curve of several blinking events (Figure 7 b) fits to previously published data [6]. But in our case we do not know in which endocytic pathway dynamin is acting. As the measured blinking events do not colocalize with caveolin, it is very likely that the observed dynamin blinking events are involved in the clathrin mediated endocytic pathway. Though they can also be acting on another pathway of endocytosis.

4.6 Future Challenges

In this study we established an assay to explore caveolar endocytosis. It will allow us to study endocytic events with a high spatial and temporal resolution using TIRF microscopy.

However, further improvements of the assay are still required. First, we have to characterize the internalization of caveolin. Then we have to determine how the caveolar pathway can be stimulated. A further goal is the identification of factors that colocalize transiently with caveolin in proximity of the plasma membrane during internalization of caveolae. If the kinetics of caveolar endocytosis can be characterized and factors can be identified this way, the role of these factors in caveolar endocytosis can be investigated.

References

[1] Dorothy A Schafer. Coupling actin dynamics and membrane dynamics during endocytosis. *Curr Opin Cell Biol*, 14(1):76–81, Feb 2002.

[2] James D Orth and Mark A McNiven. Dynamin at the actin-membrane interface. *Curr Opin Cell Biol*, 15(1):31–9, Feb 2003.

[3] Lucas Pelkmans and Ari Helenius. Endocytosis via caveolae. *Traffic*, 3(5):311–20, May 2002.

[4] D Axelrod. Total internal reflection fluorescence microscopy in cell biology. *Traffic*, 2(11):764–74, Nov 2001.

[5] JA Steyer and W Almers. A real-time view of life within 100 nm of the plasma membrane. *Nat Rev Mol Cell Biol*, 2(4):268–75, Apr 2001.

[6] Christien J Merrifield, Morris E Feldman, Lei Wan, and Wolfhard Almers. Imaging actin and dynamin recruitment during invagination of single clathrin-coated pits. *Nat Cell Biol*, 4(9):691–8, Sep 2002.

[7] Christien J Merrifield, Britta Qualmann, Michael M Kessels, and Wolfhard Almers. Neural Wiskott Aldrich Syndrome Protein (N-WASP) and the Arp2/3 complex are recruited to sites of clathrin-mediated endocytosis in cultured fibroblasts. *Eur J Cell Biol*, 83(1):13–8, Feb 2004.

[8] Y Du, SA Weed, WC Xiong, TD Marshall, and JT Parsons. Identification of a novel cortactin SH3 domain-binding protein and its localization to growth cones of cultured neurons. *Mol Cell Biol*, 18(10):5838–51, Oct 1998.

[9] Lucas Pelkmans, Daniel Püntener, and Ari Helenius. Local actin polymerization and dynamin recruitment in SV40-induced internalization of caveolae. *Science*, 296(5567):535–9, Apr 2002.

[10] Roger J Daly. Cortactin signalling and dynamic actin networks. *Biochem J*, 382(Pt 1):13–25, Aug 2004.

[11] L Pelkmans, J Kartenbeck, and A Helenius. Caveolar endocytosis of simian virus 40 reveals a new two-step vesicular-transport pathway to the ER. *Nat Cell Biol*, 3(5):473–83, May 2001.

[12] Yansong Li, Takehito Uruno, Christian Haudenschild, Steven M Dudek, Joe G N Garcia, and Xi Zhan. Interaction of cortactin and Arp2/3 complex is required for sphingosine-1-phosphate-induced endothelial cell remodeling. *Exp Cell Res*, 298(1):107–21, Aug 2004.

Appendix

A Abbreviations

AP	adapter protein
Arp3	actin related protein 3
ATCC	american type culture collection
Cav1	caveolin 1
Cttn	cortactin
DNA	desoxyribulose nucleic acid
EDTA	ethylenediaminetetraacetat, $((HOOCCH_2)_2NCH_2)_2$
EF	evanescent field
EGFP	enhanced green fluorescent protein
ER	endoplasmatic reticulum
FCS	fetal calf serum
GFP	green fluorescent protein
GPI	glycosylphosphatidylinositol
HEPES	4-(2-hydroxylethyl)-1-piperazineethanesulfonic acid
MEM	minimum essential medium
mRFP	monomeric red fluorescent protein
NA	numerical aperture
NEAA	nonessential amino acids
NTA	N-terminal acidic domain
PBS	phosphate-buffered saline
PCR	polymerase chain reaction
PIP_2	phosphatidylinositol-4,5-bisphosphate
RFP	red fluorescent protein
RGB	red green blue
SH3	Src homology 3 domain
SV40	simian virus 40
TAE	tris-acetate-EDTA
TIR	total internal reflection
TIRF	total internal reflection fluorescence
Tris	tris-(Hydroxymethyl)aminomethan, $NH_2(CH_2(OH)_3$
WASP	Wiskott-Aldrich syndrome protein